行政院國家科學委員會專題研究計畫 成果報告

室內呼吸性傳染病之傳輸潛能機率風險分析(第 2 年)
研究成果報告(完整版)

計 畫 類 別 ：個別型
計 畫 編 號 ：NSC 97-2314-B-040-006-MY2
執 行 期 間 ：98 年 08 月 01 日至 99 年 07 月 31 日
執 行 單 位 ：中山醫學大學公共衛生學系（所）

計 畫 主 持 人：陳詩潔

計畫參與人員：碩士班研究生-兼任助理人員：游舒涵

報 告 附 件 ：出席國際會議研究心得報告及發表論文

處 理 方 式 ：本計畫涉及專利或其他智慧財產權，2 年後可公開查詢

中 華 民 國 99 年 10 月 20 日

行政院國家科學委員會補助專題研究計畫 ■ 成 果 報 告
□ 期中進度報告

室內呼吸性傳染病之傳輸潛能機率風險分析

計畫類別：■ 個別型計畫　□ 整合型計畫
計畫編號：NSC 97 － 2314 － B － 040 － 006 － MY2
執行期間：　97 年 08 月 01 日至 99 年 07 月 31 日

計畫主持人：陳詩潔
共同主持人：
計畫參與人員： 兼任助理 碩士班研究生 游舒涵

成果報告類型(依經費核定清單規定繳交)：□精簡報告 ■完整報告

本成果報告包括以下應繳交之附件：
□赴國外出差或研習心得報告一份
□赴大陸地區出差或研習心得報告一份
■出席國際學術會議心得報告及發表之論文各一份
□國際合作研究計畫國外研究報告書一份

處理方式：除產學合作研究計畫、提升產業技術及人才培育研究計畫、列管計畫及下列情形者外，得立即公開查詢
□涉及專利或其他智慧財產權，□一年■二年後可公開查詢

執行單位：中山醫學大學公共衛生學系

中 華 民 國 99 年 10 月 09 日

行政院國家科學委員會專題研究計畫期中報告
室內呼吸性傳染病之傳輸潛能機率風險分析(2/2)

計畫編號：NSC 97－2314－B－040－006－MY2
執行期限：97/08/01~99/07/31
執行單位：中山醫學大學公共衛生學系
主 持 人：陳詩潔

摘要

本計畫提供一個預測性模式以模擬易感族群之流感傳輸潛能，以整合流感病毒動態模式、室內氣膠傳輸模式及飛沫粒徑分佈特性。藉由流感病毒動態模式，人體宿主和病原體之間交互作用可分為三個等級，包括(A)上皮細胞等級、(B)人體免疫反應等級與(C)病毒等級，可評估每日時變的病毒力價產生率與飛沫粒徑大小；進而利用 Wells-Riley 方程式推求重要的參數感染風險(P)和基本再生數(R_0)以量化流感傳輸潛能。結果顯示，A 型(H1N1)流感反應第一個的是干擾素(i)，開始於病毒產生兩個小時內，並於感染後第三至第四天間達到高峰，而毒殺性 T 細胞(Z)反應較慢，於感染後第十天達到高峰。然而，在病毒層級中，病毒力價在感染後第二天達最大值，第七天達到 5.96×10^9 的 virions 病毒粒子數。靈敏度分析得知，受感染細胞產生病毒之速度(k) = 4000 d^{-1} infected $cell^{-1}$ 與未受感染上皮細胞感染率(β) = 5×10^{-10} d^{-1} $virion^{-1}$ 使實驗性人體感染數據和模式預測相關性達顯著(r = 0.99, p < 0.0001)，顯示 β 在病毒動態中扮演重要的角色。結果指出流感病毒感染速率 P 和 R_0 的中位數和 95%信賴區間分別為 0.132 (0.09 – 0.19) 和 1.19 (0.76 – 1.86)。潛在的流感病毒傳輸可藉由 $R_0>1$ 判斷。建議預測的模式可作為進一步具體調查控制策略的工具，例如個人防護面罩去改變顆粒大小和數量濃度特徵以及減少呼出飛沫以降低室內環境中的感染風險。

關鍵詞：流感，傳染風險，病毒動態，液滴，模式，公共衛生。

Abstract

This proposal provides a predictive model that can integrate the modified influenza A (H1N1) virus dynamic model, indoor aerosol transmission model, and characterizing the droplet size distribution to estimate the transmission potential in a proposed susceptible population. By studying the influenza virus dynamic model, we explored the consequences of host-pathogen interactions involving in three levels: (A) epithelial cell level, (B) human immune response level, and (C) virus level. To evaluate the quantum generation rate varying with the day post infection and pathogen-carrying particle diameter, and to quantify exhaled bioaerosol infections for the critical key parameters of risk of infection (P) and basic reproduction number (R_0) based on Wells-Riley mathematical equation. Results show that the first responder to influenza A infection was interferon molecules (i) that the production began less than 2 h after viral introduction, and then reached a peak between days 3 – 4. The cytotoxic T-cell (Z) responder was much slower with a CTL activity peak at day 10. However, in virus level, a large number of virus concentrations appeared at day 2 and reached to a peak value of 5.96×10^9 virons at day 7. Sensitivity analysis indicated that input values of Creation rate of viruses by an infected epithelial cell (k) = 4000 d^{-1} infected $cell^{-1}$ and infection rate of an unprotected epithelial cell (β) = 5×10^{-10} d^{-1} $virion^{-1}$ resulted in a significant correlation between experimental human infection data and model predictions (r = 0.99, p < 0.0001), suggesting that β has an important role involved in the virus dynamics. The result indicated that the box and whisker plots of median with 95% CI of P and R_0 were estimated to be 0.132 (0.09 – 0.19) and 1.19 (0.76 – 1.86) for influenza viruses. The potential transmission of infection for influenza viruses can be judged by $R_0>1$. The proposed predictive model may serve as a tool for further investigation of specific control measure such as the personal protection masks to alter the particle size and number concentration characteristics and minimize the exhaled bioaerosol droplet to decrease the infection risk in indoor environment settings.

Key words: Influenza; Transmission risk; Virus dynamics; Droplet; Modeling; Public Health.

Introduction

A variety of mathematical and computational models have been proposed for elucidating the nonlinear transmission dynamics of epidemics and for enhancing our understanding of the within-host spread of diseases and the immune response (Nowak and May, 2000; Perelson, 2002; Van Kerkhove et al., 2010). Important results have been obtained from the mathematical modeling of virus dynamics for the HIV (Perelson et al., 1996; 1997; Nowak and Bangham, 1996), hepatitis B virus (HBV) (Marchuk et al., 1991; Nowak et al., 1996), hepatitis C (Neumann et al., 1998) and influenza infections (Baccam et al., 2006; Hancioglu et al., 2007; Chang and Young, 2007).

When influenza virus infected a healthy person, there are many complex factors governing the process of influenza infection, the multiple mechanisms were interacted among immunology, cells dynamics, and virus generation rate. Computer simulation would be a useful tool to independently dissect the potential contribution and relative importance of each factor or to investigate unexpected scenarios that are difficult to replicate experimentally.

Viral kinetics can be used to express the competed results of human immunity ability with influenza virus generation. Baccam et al. (2006) provided two models describing the kinetics of influenza A virus infection in human: a target cell-limited model and a target cell-limited model with delayed virus production. They used data from experimentally infected volunteers to estimate the reasonable parameters of biological characteristics appeared in the models. Their findings suggested that the model considering the delayed virus production was more realistic because of the infected cells begin producing influenza virus for nearly 5 hours. Chang and Young (2007) developed a simple scaling law-based ordinary differential model for describing the time courses of the numbers of infectious viral particles, activated cytotoxic T-lymphocytes, interferon molecules, infected cells, uninfected cells, and the subset of uninfected cells that are protected by interferon from viral infection. They found that the rise time, duration, and the severity of the influenza A infection could be expressed as a function of the initial viral load and the relevant parameters based on the developed scaling laws.

Experimental human influenza A virus infection can provide the local and systemic cytokine responses during the infection period (Hayden et al., 1998), even the safety and efficacy of the oral or intravenous neuraminidase inhibitor (Hayden et al., 1999; Hayden et al., 1996; Fritz et al., 1999; Calfee et al., 1999). Different experimental trails for assessing the dose, form, and the challenge's responses include daily viral titer, shedding virus, peak titer, days of shedding, and clinical symptom scores. Hence, by using the experimental human infection data to validate the viral dynamic models leads to increase the accuracy of the model prediction and a comparison of parameter sensitive analysis can also be achieved.

Transmission of exhaled infectious droplets in the indoor environment has been receiving substantial attentions. Duguid (1946) indicated that the lognormal distribution could best describe the respiratory droplet with a geometric mean (GM) 14 μm and a geometric standard deviation (GSD) 2.6 for cough and a GM 8.1 μm and a GSD 2.3 for sneeze. Papineni and Rosenthal (1997) measured expired bioaerosol droplets (in nose and mouth breathing, coughing and talking) to be less than 2 μm in size, with no droplets larger than 8 μm. Hence, the particle size distribution may play a key role for evaluating the infection risk.

Hence, in this study, we sought to develop a mathematical model by combining a target cell-limited model with delayed virus production by Baccam et al. (2006) and a reduced population dynamic model of immune response by Chang and Young (2007). More importantly, the modified influenza virus dynamic model was used to explore the sensitive analysis and to perform the model validation against the experimental human infection data within an individual. We believed that this present framework could be

incorporated explicitly into control measure modeling schemes.

Materials and Methods

Mathematical model of modified influenza virus dynamics

By studying a model of influenza virus dynamics that builds on past well-developed models of Baccam et al. (2006) and Chang and Yang (2007), we explored the consequences of host-pathogen interactions involving in three levels: (i) epithelial cell level, (ii) human immune response level, and (iii) virus level. The essential features of the present model are depicted in Fig. 1. The roles of immune response properties of epithelial cells act as the interferon (IFN) and cytotoxic T-lymphocytes (CTLs) immunity.

Briefly, in epithelial cell level (Fig. 1A), uninfected cells (X) can be infected by free virus particles (V) and can transmit to infected cells (Y). During the virus transform and replication by cell DNA, Y will take almost 6 to 8 hr for transmission to the state of producing virus infected cells (J). In human immune response level (Fig. 1B), cytotoxic T-cell (Z) can be induced and activated by infected cells (Y) and produced virus infected cells (J). Interferon molecules (i) also play the role in immune response mechanism and can protect cells (X_R) from increasing infected cells. The present model used the free virions in epithelial cells (V) to represent the virus level (Fig. 1C).

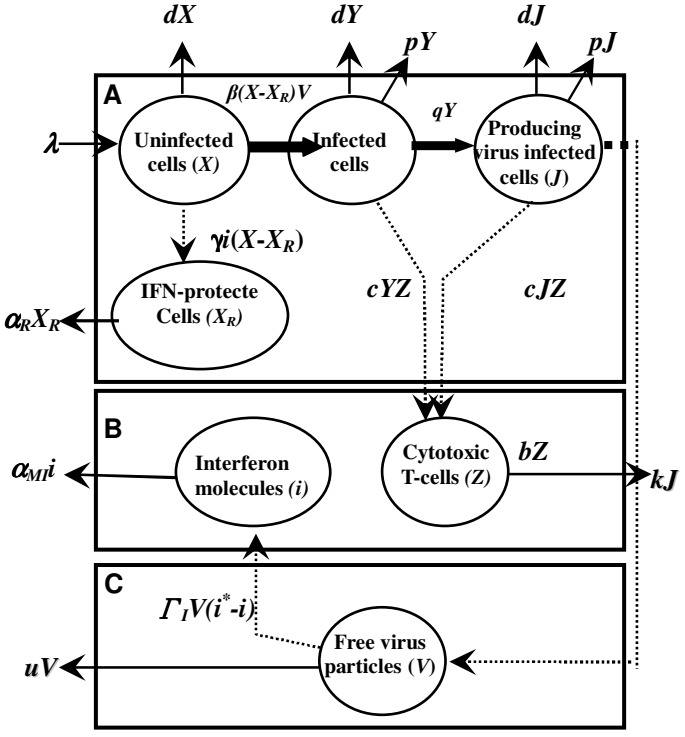

Fig. 1. Schematic representation showing the interaction pathways of influenza virus infects human lung epithelial cell among (A) epithelial cell level, (B) human immune response level, and (C) virus level. The definition of symbols and detailed descriptions are explained in texts and Table 1.

The system of ordinary differential equations corresponding to the model in Fig. 1 and based on previous work (Baccam et al., 2006; Chang and Yang, 2007) is as follows,

$$\frac{dX}{dt} = \lambda - dX - \beta(X - X_R)V, \quad (1)$$

$$\frac{dY}{dt} = \beta(X - X_R)V - aY - qY - pYZ, \quad (2)$$

$$\frac{dJ}{dt} = qY - aJ - pJZ, \quad (3)$$

$$\frac{dV}{dt} = kJ - uV, \quad (4)$$

$$\frac{dZ}{dt} = c(Y + J)Z - bZ, \quad (5)$$

$$\frac{dX_R}{dt} = \gamma i(X - X_R) - \alpha_R X_R, \quad (6)$$

$$\frac{di}{dt} = \Gamma_I V(i^* - i) - \alpha_{MI} i, \quad (7)$$

where λ is the equilibrium creation rate of epithelial cells (d^{-1}); β is the infection rate of an unprotected epithelial cell per virion (d^{-1} $virion^{-1}$); a is the reciprocal of infected epithelial cell lifetime (d^{-1}); q is the transition rate from Y to J (d^{-1}); p is the infected epithelial cell CTL-induced destruction rate (d^{-1} CTL^{-1}); k is the creation rate of viruses by an infected epithelial cell (d^{-1} infected $cell^{-1}$); u is the reciprocal of influenza A virus lifetime (d^{-1}); c is the CTL-induced creation rate of CTL per infected epithelial cell (d^{-1} infected $cell^{-1}$); b is the reciprocal of CTL lifetime (d^{-1}); γ is the rate constant for induction of resistive state by IFN (inflamed) (d^{-1} IFN^{-1}); α_R is the rate of virus resistant epithelial cell decay (d^{-1}); Γ_I is the induction rate for IFN production (d^{-1} $virion^{-1}$); i^* is the effective creation rate number for IFN; and α_{MI} is the rate of loss of IFN-producing macrophages (d^{-1}). Model simulations were performed by using ode45 solver in MATLAB (The MathWorks Inc., Natick, Massachusetts, USA).

Parameter estimation and sensitivity analysis

The definition, symbols, input values, and expected physiological ranges of parameters in the present modified influenza virus dynamic model were summarized in Table 1. The input parameters of biological characteristics were derived from experimentally infected volunteers (Murphy et al., 1980; Bocharov and Romanyukha, 1994, Beauchemin et al, 2005) in that the physiological ranges for individual differences can also be estimated.

To identify the most significant sensitive parameters in this modified influenza virus dynamic model, we performed a sensitivity analysis for four parameters involving creation rates λ and k with infection rate β and transition rate q, respectively. This qualitative analysis can show robustness of the effects of free virons dynamics to variations in key parameters and model assumptions. The sensitivity analysis was performed by varying the key creation and destruction rates of λ, q, k, and β ranged from $0 - 6.57\times10^{7}$ d^{-1}, $2 - 6$ d^{-1}, $67 - 6700$ d^{-1} infected $cell^{-1}$, and $3\times10^{-14} - 6\times10^{-10}$ d^{-1} $virion^{-1}$, respectively.

Experimental influenza infection survey for model validation

To perform the model validation, 10 published experimental influenza infection studies were used as the study data. Briefly, the participants were inoculated intranasally (0.25 ml per nostril) with inoculation dose ranged from $10^{4.5}$ to 10^{7} tissue culture infected dose ($TCID_{50}$) of H1N1 virus on day 0. Nasal washings were collected before viral inoculation for detection of virus infection and collected (days 0, 1, 2, 3, 4, 5, 6, 7 and 8) for virus isolation.

Table 1. Definition, symbols, input values, and expected physiological ranges of parameters in the present modify influenza virus dynamic model

Symbols	Definition (unit)	Input values[b]	Range[a]
X_0	Equilibrium number of normal epithelial cells in upper six branches (#)	10^{9}	-
λ	Equilibrium creation rate of epithelial cells (d^{-1})	6.25×10^{7}	-
d	Reciprocal of epithelial cell lifetime (d^{-1})	0.0625	-
β	Infection rate of an unprotected epithelial cell per virion (d^{-1} $virion^{-1}$)	10^{-10}	$3\times10^{-14} - 6\times10^{-10}$
a	Reciprocal of infected epithelial cell lifetime (d^{-1})	1	0.5-2
q	Transition rate from Y to J (d^{-1})	4[c]	2 – 6[c]
p	Infected epithelial cell CTL-induced destruction rate (d^{-1} CTL^{-1})	10^{-10}	$4\times10^{-12} - 5\times10^{-10}$
V_0	Initial virus particles (virions)	10^{7}	-
k	Creation rate of viruses by an infected epithelial cell (d^{-1} infected $cell^{-1}$)	340	67 – 6700
u	Reciprocal of influenza A virus lifetime (d^{-1})	2	2 – 4
Z_0	Initial number of influenza A specific CTLs in upper six branches (#)	7×10^{6}	$0.72\times10^{6} - 7.2\times10^{6}$
c	CTL-induced creation rate of CTL per infected epithelial cell (d^{-1} infected $cell^{-1}$)	3.6×10^{-8} [a]	-
b	Reciprocal of CTL lifetime (d^{-1})	0.5	-
γ	Rate constant for induction of resistive state by IFN (inflamed) (d^{-1} IFN^{-1})	10^{-9}	$10^{-8} - 10^{-10}$
α_R	Rate of virus resistant epithelial cell decay (d^{-1})	1	-
Γ_I	Induction rate for IFN production (d^{-1} $virion^{-1}$)	8×10^{-10}	-
i^*	Effective creation rate number for IFN	10^{10}	$7.7\times10^{7} - 7.7\times10^{10}$
α_{MI}	Rate of loss of IFN-producing macrophages (d^{-1})	0.5	0.3 – 0.5

[a]All of the estimated physiological ranges shown are based on the parameter estimates in Bocharov and Romanyukha (1994), except for the value of c which was directly obtained from Beauchemin et al. (2005).
[b]Adopted from Murphy et al. (1980)(cited in Chang and Young (2007)).
[c]Adopted from Baccam et al. (2006)

The age group, size of study subgroups, the number of infected population, even the number of shedding virus and shedding durations were all recorded. We estimated the daily-based average viral titers ($logTCID_{50}$ ml^{-1}) based on the published study data at

specific day 0 (time for inoculating) to day 8. Statistical analysis was performed by using free virions of the present modified virus dynamics and daily-based average viral titers based on the experimental influenza infections.

The data management and statistical analyses were performed by using SAS Version 9.1.3 for Windows (SAS Institute Inc., Cary, North Carolina, USA). Diger 4 software (Golden Software Inc., Golden, Colorado, USA) was used for data collection from the published studies.

Quantum generation rate for different influenza subtype

In this study, the "infectious dose" for influenza (sub)type viruses is quantified by the concept of "quantum" that was emitted by an infected person. For estimating quantum for influenza (sub)type viruses, we adapted the concept based on Nicas et al. (2005) by quantifying the risk of secondary airborne infection by the characteristics of emission of respiratory pathogens. Hence, we considered two parameters of particle size diameter and the day post infection that might impact the quantum estimations. We focused on the particle size diameter ≤ 10 μm to estimate the airborne infection (Duguid, 1946, Loudon and Robert, 1967) and defined the quantum as,

$$q(t,x) = E \times C_t \times N_x \times \overline{v}_x , \quad (8)$$

where $q(t, x)$ is the quantum generation rate varying with the day post infection (t) and particle size diameter x ($x \le 10\,\mu m$) (TCID50 h^{-1}), E is the expulsion event rate by sneeze (event hr^{-1}), C_t is the influenza (sub)type viruses shedding in respiratory fluid (TCID50 ml^{-1}), N_x is the particle number concentration in each particle size diameter x (ml^{-1}), and $\overline{v}_x$ is the particle volume per expulsion event (ml).

The best fitted model for viral shedding of influenza H1N1 viruses were obtained from experimental data (Carrat et al., 2008) in that influenza data were provided by 116 participants who shed influenza viruses. The sum of the total particle volume at specific particle size diameter x can be expressed as $N_x \times \overline{v}_x$. We adopted the valuable experimental data from Duguid (1946) to describe the relationship between particle size diameter and droplet number concentration of sneeze. The relationship between particle initial volume and number of particles emitted per sneeze was adopted from Loudon and Roberts (1967).

Wells-Riley mathematical equation

The Wells-Riley mathematical equation was used to estimate indoor airborne infection risk in an enclosed space. Riley and Nardell (1989) made two assumptions to quantify the indoor respiratory infections. The first assumption implies that an infectious droplet nucleus has an equal chance of being anywhere within a building's airspace. The second assumption implies that the quantum concentration and the outdoor air supply rate remain constant with time.

We modified the Wells-Riley mathematical equation to estimate the transmission potential of influenza viruses in a hospital setting,

$$P = \frac{D}{S} = 1 - \exp\left\{ -\frac{I q_{\max} p t}{Q} \left\{ 1 - \frac{V}{Qt}\left[1 - \exp\left(-\frac{Qt}{V} \right) \right] \right\} \right\} \quad (9)$$

where P is the probability of infection for susceptible population varied with influenza viruses, D is the number of cases among S persons susceptible to the infection, S is the number of susceptible, I is the number of sources of infection, $q_{\max}$ expressed the maximum value of our modeling results of $q(t,x)$ (TCID50 h^{-1}), p is the pulmonary ventilation rate of susceptible individuals (m^3 d^{-1}), t is the exposure time (d), Q is the fresh air supply rate that removes the infectious aerosol in volume per unit of time (m^3 h^{-1}), and V is the volume of the ventilated space (m^3). For modeling the respiratory infection, we incorporate initial I =1 and $S = n - 1$ into Eq. (9) to estimate basic reproductive number (R_0) for quantifying the average number of successfully secondary infection cases generated by a typical primary infected case in an entirely susceptible population,

$$R_0 = (n-1)\left\{1-\exp\left\{-\frac{q_{\max}\, pt}{Q}\left\{1-\frac{V}{Qt}\left[1-\exp\left(-\frac{Qt}{V}\right)\right]\right\}\right\}\right\} \quad (10)$$

where the symbol of n represents the total number in our modeling ventilation airspaces. The R_0 of different influenza viruses thus can be estimated by using Eq. (10).

Results and discussion

Influenza virus dynamics

We found that uninfected cells (X) decreased by free virus infection from the initial values of 10^9 cells; then IFN-protected cells (X_R) increased rapidly at days 2 – 3 and reached a peak value of 8.2×10^8 cells at day 3.4, showing the 89% protection by interferon at that moment (Fig. 2A). On the other hand, the peak values of infected cells (Y) and producing virus infected cells (J) occurred at days 2.5 and 7 with 9.55×10^6 cells and 3.54×10^7 cells, respectively (Fig. 2A).

In human immune response level, the first responder to influenza A infection was interferon molecules (i) that the production began less than 2 h after viral introduction, and then reached a peak between days 3 – 4 (Fig. 2B). The cytotoxic T-cell (Z) responder was much slower with a CTL activity peak at day 10 (Fig. 2B). In virus level, a large number of virus concentration appeared at day 2 and reached to a peak value of 5.96×10^9 virons at day 7 (Fig. 2C). Our simulations showed that the virus replication in human epithelial lung cells was much more rapid than that of initial viral load at $V_0 = 10^7$ virons.

Human experimental viral titer concentration

Table 2 summaries the experimental human influenza A (H1N1) infection data. The test age groups were young health man and women in that the number of infected population ranged from 8 – 59 persons with shedding durations ranged from 2 – 5.1 days. In order to estimate the daily-based average viral titers, we used approximate values for Barroso et al. (2005). The overall patterns started after day 1 and approached to peak viral titers during day 2 with $10^{3.51}$ $TCID_{50}$ ml^{-1} then slowly decreased to less than 10^1 $TCID_{50}$ ml^{-1} at day 6.

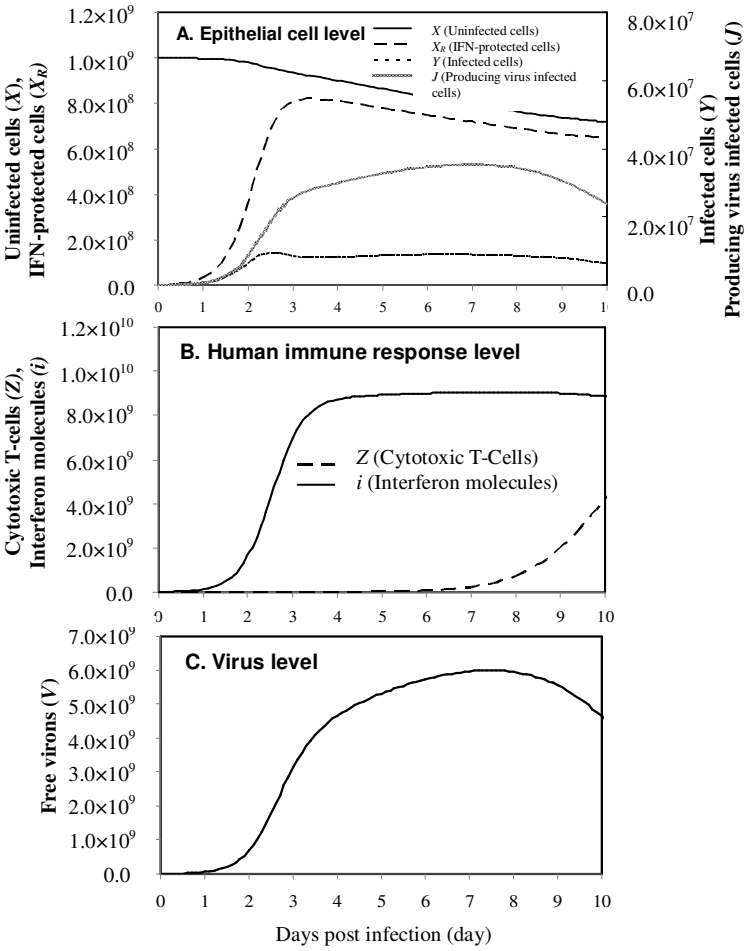

Fig. 2. Model influenza A variables in the three levels among (A) X (uninfected cells), X_R (IFN-protected cells), Y (infected cells), and J (producing virus infected cells) in epithelial cell level, (B) Z (cytotoxic t-cells) and I (interferon molecules) in human immune response level, and (C) V (viral titers) with an initial viral load of 10^7 virons. Input values of parameters are presents in Table 1.

Sensitivity analysis

To evaluate the variability of parameters that significantly contribute to the free virons, sensitivity analyses were performed. The time course of free virons was used to show the model sensitivity to variations in parameters k, and β, respectively, (Fig. 3). We found that the infection rates of an uninfected cell to infected cells increased with increasing the input parameters of infection rate β from 6×10^{-10} to 3×10^{-14} d^{-1} $virons^{-1}$. Similarly, free virons in epithelial cell increased with increasing the value of creation rate of virus by an infected epithelial cell k (Fig. 3).

Here Pearson correlation analysis was used to determine the optimal parameter

inputs with best statistical significances between the daily-based average viral titers and the prediction of free virons that varied with physiological ranges of parameter. Our results indicated that input values of k = 4000 and $\beta = 5\times10^{-10}$ resulted in a significant correlation between experimental human infection data and model predictions (r = 0.99, $p < 0.0001$) (Table 3).

This sensitivity analysis thus suggested that infection rate of an unprotected epithelial cell (β) has an important role involved in the virus dynamics, whereas creation rate of virus by an infected epithelial cell (k) is the second sensitive parameter to the model.

Table 2. *Summary of experimental human influenza A (H1N1) infection data*

Age group	Size of study subgroups (n_i)	Virus	Inocul. Dose ($TCID_{50}$)	Infected N (% of subgroup size)	Shedding virus N (% of infected)	Mean virus shedding duration (day)	Reference
18-25	9	A/California/10/78/H1	$10^{4.5}$	8 (89)	8 (100)	NA	Treanor et al. (1987)
18-45	16	A/Kawasaki/86/H1N1	10^{7}	16 (100)	16 (100)	2.8	Hayden et al. (1994)
18-33	59	A/Texas/91/H1N1	10^{5}	49 (83)	49 (100)	2	Hayden et al. (1996)
19-40	19	A/Texas/36/91/H1N1	10^{5}	19 (100)	19 (100)	NA	Hayden et al. (1998)
18-40	14	A/Texas/36/91/H1N1	10^{6}	14 (100)	14 (100)	NA	Murphy et al. (1998)
19-33	8	A/Texas/36/91/H1N1	10^{5}	8 (100)	8 (100)	4.6	Fritz et al. (1999)
19-35	8	A/Texas/36/91/H1N1	10^{5}	8 (100)	8 (100)	NA	Calfee et al. (1999)
18-40	13	A/Texas/36/91/H1N1	10^{6}	13 (100)	NA	4.5	Hayden et al. (1999)
19-40	14	A/Texas/36/91/H1N1	10^{5}	14 (100)	14 (100)	5.1	Kaiser et al. (1999)
18-45	18	A/Texas/36/91/H1N1	10^{6}	17 (94)	17 (100)	3.2	Barroso et al. (2005)

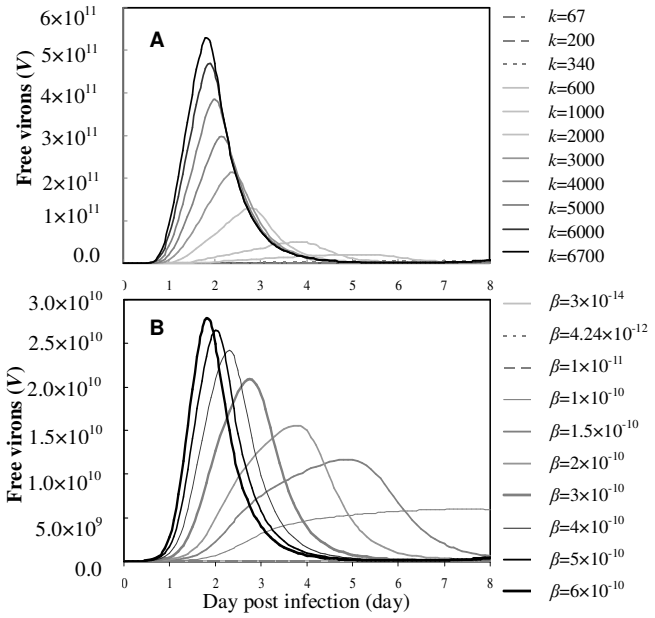

Fig. 3. Sensitivity analysis of λ (equilibrium creation rate of epithelial cells (d^{-1})), q (transition rate from Y to J (d^{-1})), k (creation rate of viruses by an infected epithelial cell (d^{-1} infected $cell^{-1}$)) and β (Reciprocal of epithelial cell lifetime (d^{-1})) are presented. The expected physiological ranges of those four parameters are present in Table 1.

Table 3. Optimal Pearson correlation analysis between experimental human infection data and modeling results of modified virus dynamic model

Parameter	Input value (Original value)	Optimal r	p-value
λ	6.25×10^{7} (6.25×10^{7})	- 0.43	0.2459
q	2 (4)	- 0.46	0.2077
k	4000 (340)	0.996	< 0.0001
β	5×10^{-10} (10^{-10})	0.999	< 0.0001

Model validation

To test this prediction, we performed the model validation with derived optimal estimates of creation rate k and infection rate β values. Fig. 4A shows the time course of predicted free virons in epithelial cell with the optimal parameters of k = 4000 and β = 5×10^{-10} against the experimental data of daily-based average viral titers. Generally, the results were in agreement with the experimental data trend, except on days 6 – 8 where the data experienced a decreasing fashion. Furthermore, this study also compared the predictive capacities among the free virons among target-cell limited model with delay virus production (Baccam et al., 2006), the immune response model (Chang and Young, 2007), and our modified virus dynamic model (Fig. 4B). Our results indicated that the best-fitted time course of simulated free virons by the present modified virus dynamic model well captured the observed dynamics (r^2 = 0.99, p < 0.0001) than those of the target-cell limited model with delay virus production (r^2 = 0.85, p = 0.0004) and the immune response model (r^2 < 0.1, p = 0.955) (Fig. 4B). Therefore, the performance of the published models was relative lower than that of the present proposed model as revealed by model comparisons against the experimental data.

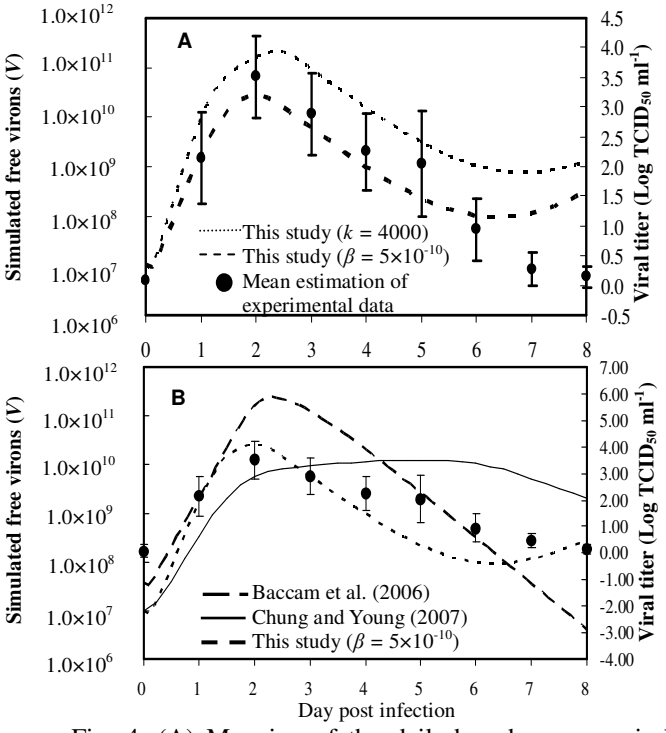

Fig. 4. (A) Mapping of the daily-based average viral titers and simulated free virons for model validation. (B) Furthermore, this study compares the prediction accuracy of free virons among target-cell limited model with delay virus production (Baccam et al., 2006), immune response model (Chang and Young, 2007), and our modified model.

Quantum generation rate varied with influenza virus

Fig. 5A indicates the relationship between particle size diameter and particle number for sneeze that adopted from Duguid et al. (1946). Moreover, Fig. 5B shows the correlation between the particle size diameter and size-dependent total particle volume that adopted from Loudon and Roberts (1967). The analysis of the time-dependent virus concentration in respiratory fluid (C_t) revealed that the influenza A (H1N1) curve sharply increased at day 1, reached the maximum values during the day 2, and return to the basic values at days 7 to 8 (Figs. 5A, 3C). Hence, we integrated the frequency of sneeze per hour (E) with E = 5 h^{-1}, time-dependent virus concentration in respiratory fluid for influenza viruses, and size-dependent total particle volume to simulate the dynamics of quantum generation rate ($q(t,x)$).

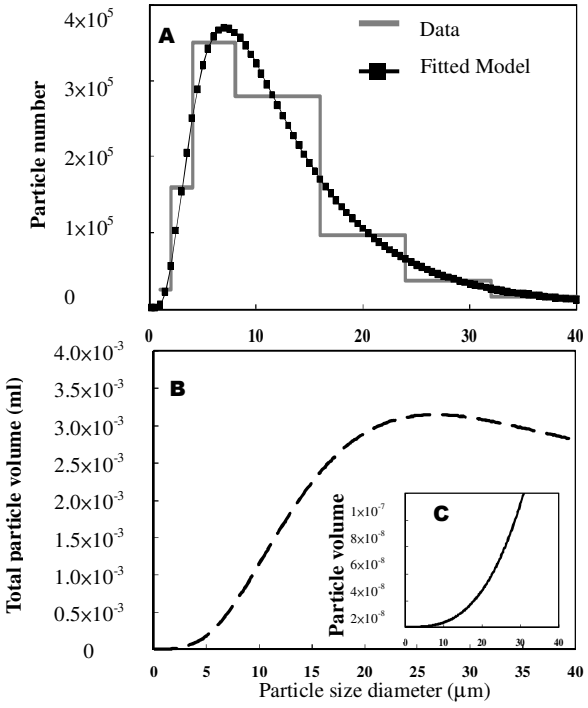

Fig. 5. (A) The original experimental data fro sneeze from Duguid (1946) shows the relationship between particle size diameter and particle number concentration. (B) The size-dependent total particle

volume for sneeze which are estimated by Fig. 2A and Fig. 2C, in that (C) was the best fitted model to the data Duguid (1946) and describing the relationship between the particle size diameters corresponding to the particle initial volume per sneeze from diameter 0 to 40 μm.

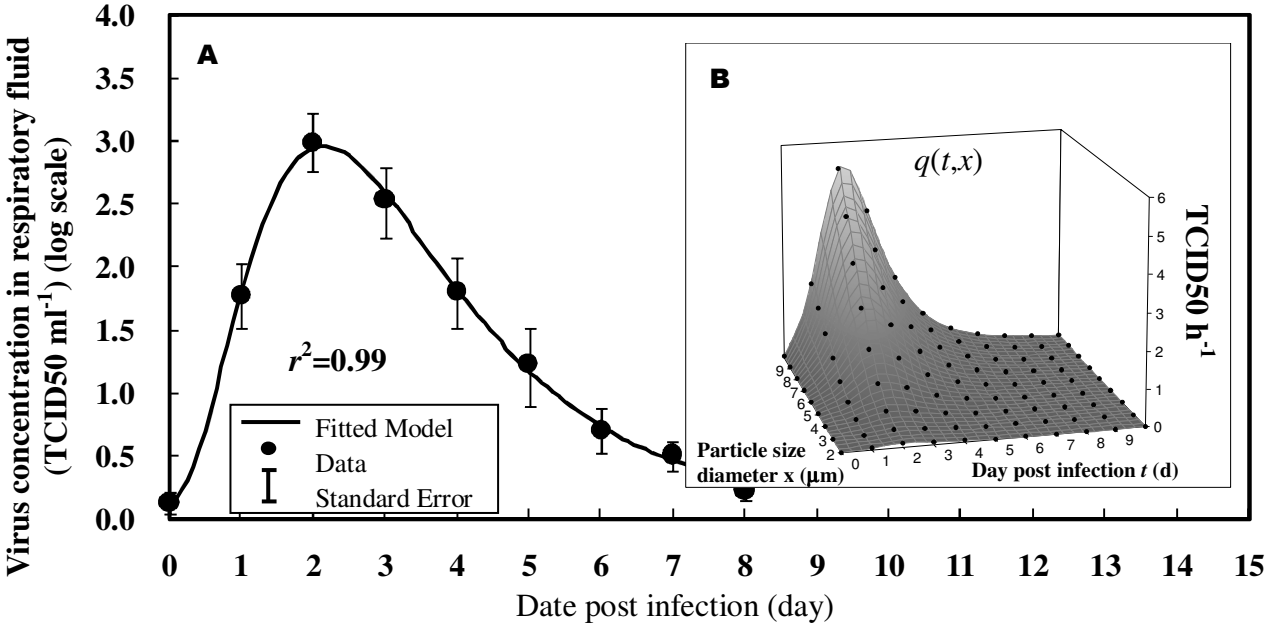

Fig. 6. Panels A, C, and E represented the viral dynamics of influenza A subtype H1N1, subtype H3N2, and influenza B viruses, respectively. Panels B, D, and F illustrate the quantum generation rate $q(t,x)$ for sneeze events in which t represents the number of days after infection (day) and x expresses the particle size diameter (μm).

Fig. 6B revealed the interesting response surface of the influenza type-specific quantum generation rate by Eq. (8). This results indicate that the maximum quantum generation rate (q_{max}) is estimated to be 5.25 TCID50 h^{-1} (at x = 10 μm, day 2 post infection) for influenza A (H1N1). The size-dependent particle number concentration of sneeze activity may explain why the q_{max} all appeared at the particle size diameter x = 10. Observably, the exhaled particle number almost attended to 3×10^5 – 4×10^5 for one sneeze (Fig. 6A).

Risk of infection and basic reproduction number

Based on Eqs. (9) and (10), R_0 in Wells-Riley mathematical equation can be estimated. The result indicates that the box and whisker plots of median with 95% CI of risks of infection (P) and basic reproduction numbers (R_0) are estimated to be 0.132 (0.09 – 0.19), 1.19 (0.76 – 1.86) for A (H1N1) (Fig. 7). Potential transmission infection of three influenza viruses can be judged by $R_0 > 1$.

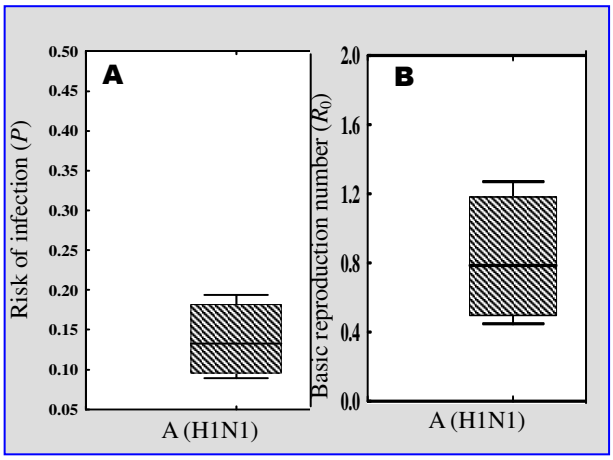

Fig. 7. The box and whisker plots of (A) the risk of infection (P) and (B) basic reproduction number (R_0) for influenza A subtype H1N1, respectively.

Reference

1. Baccam P, *et al.* Kinetics of influenza A virus infection in humans. *Journal of Virology* 2006; 80: 7590–7599.
2. Barroso L, *et al.* Efficacy and tolerability of the oral neuraminidase inhibitor peramivir in experimental human influenza: randomized, controlled trails for prophylaxis and treatment. *Antiviral Therapy* 2005; 10: 901–910.

3. Calfee DP, *et al.* Safety and efficacy of intravenous zanamivir in preventing experimental human influenza A virus infection. *Antimicrobial Agents and Chemotherapy* 1999; 43: 1616–1620.
4. Carrat F, *et al*. Time lines of infection and Disease in Human Influenza: A review of volunteer challenge studies. *American Journal of Epidemiology* 2008; 167: 775–785.
5. Chang DB, Young CS. Simple scaling laws for influenza A rise time, duration, and severity. *Journal of Theoretical Biology* 2007; 246: 621–635.
6. Diger® Version 4. Golden Software.
7. Duguid JP. The size and distribution of air-carriage of respiratory droplets and droplet-nuclei. *Journal of Hygiene* 1946; 4: 471–480.
8. Fritz RS, *et al.* Nasal cytokine and chemokine responses in experimental influenza A virus infection: results of a placebo-controlled trial of intravenous zanamivir treatment. *The Journal of Infectious Diseases* 1999; 180: 586–593.
9. Hancioglu B, Swigon D, Clermont G. A dynamical model of human immune response to influenza A virus infection. *Journal of Theoretical Biology* 2007; 246: 70–86.
10. Hayden FG, *et al.* Local and systemic cytokine response during experimental human influenza A virus infection. *The Journal of Clinical Investigation* 1998; 101: 643–649.
11. Hayden FG, *et al.* Oral LY217896 for prevention of experimental influenza A virus infection and illness in humans. *Antimicrobial Agents and Chemotherapy* 1994; 38: 1178–1181.
12. Hayden FG, *et al.* Safety and efficacy of the neuraminidase inhibitor GG167 in experimental human influenza. *The Journal of the American Medical Association* 1996; 275: 295–299.
13. Hayden FG, *et al.* Use of the oral neuraminidase inhibitor oseltamivir in experimental human influenza. *The Journal of the American Medical Association* 1999; 282: 1240–1246.
14. Hayden FG, *et al.* Local and systemic cytokine response during experimental human influenza A virus infection. *Journal of Clinical Investigation* 1998; 101: 643–649.
15. Kaiser L, Briones MS, Hayden FG. Performance of virus isolation and directigen flu A to detect influenza A virus in experimental human infection. *Journal of Clinical Virology* 1999; 14: 191–197.
16. Loudon RG, Roberts RM. Relation between the airborne diameters of respiratory droplets and the diameter of the stains left after recovery. *Nature* 1967; 213: 95–96.
17. Marchuk GI, *et al.* Mathematical model of antiviral immune response. I. Data analysis, generalized picture construction and parameters evaluation for hepatitis B. *Journal of Theoretical Biology* 1991; 151: 1–40.
18. Murphy AW, *et al.* Respiratory nitric oxide levels in experimental human influenza. *Chest* 1998; 114: 452–456.
19. Murphy BR, Rennels MB, Douglas RG. Evaluation of influenza A/Hong Kong/123/77(H1N1) *ts*-1A2 and cold-adapted recombinant viruses in seronegative adult volunteers. *Infection and Immunity* 1980; 29: 348–355.
20. Neumann AU, *et al.* Hepatitis C viral dynamics in vivo and the antiviral efficacy of interferon-alpha therapy. *Science* 1998; 282: 103–107.
21. Nicas M, Nazaroff WW, Hubbard A. Toward understanding the risk of secondary airborne infection: emission of respiratory pathogens. *Journal of Occupational and Environmental Hygiene* 2005; 2: 143–154.
22. Nowak MA, Bangham CRM. Population dynamics of immune responses to persistent viruses. *Science* 1996; 272: 74–79.
23. Nowak MA, *et al.* Viral dynamics in hepatitis B virus infection. *Proceedings of the National Academy of Sciences of the United States of America* 1996; 93: 4398–4402.
24. Nowak MA, May RM. "Virus dynamics," Oxford University Press, Oxford, United Kingdom, 2000.
25. Papineni RS, Rosenthal FS. The size

distribution of droplets in the exhaled breath of healthy human subjects. *Journal of Aerosol Medicine* 1997; 10: 105–116.
26. Perelson AS, *et al.* Decay characteristics of HIV-1-infected compartments during combination therapy. *Nature* 1997; 387: 188–191.
27. Perelson AS, *et al.* HIV-1 ynamics in vivo: viron clearance rate, infected cell life-span, and viral generation time. *Science* 1996; 271: 1582 – 1586.
28. Perelson AS. Modelling viral and immune system dynamics, *Nature Reviews Immunology* 2002; 2: 28–36.
29. Riley RL, Nardell EA. Clearing the air. The theory and application of ultraviolet air disinfection. *American Review of Respiratory Disease* 1989; 139: 1286–1294.
30. Treanor JJ, *et al.* Intranasally administered interferon as prophylaxis against experimentally induced influenza A virus infection in humans. *The Journal of Infectious Diseases* 1987; 156: 379–383.
31. Van Kerkhove MD, *et al.* Studies needed to address public health challenges of the 2009 H1N1 influenza pandemic: Insights from modeling. *PLoS Medicine* 2010; 7: e1000275.

本計畫發表 SCI

Szu-Chieh Chen, Chung-Min Liao. 2010. Probabilistic indoor transmission modeling for influenza (sub)type viruses. ***Journal of Infection*** 60(1): 26-35. (SCI) (IF=3.060, Ranking in Infectious Diseases = 15/57 = 26.32%)

Szu-Chieh Chen, Shu-Han You, Ching-Yi Liu, Chia-Pin Chio, Chung-Min Liao*. 2011. A parsimonious viral dynamic model in epithelial cells enhances mechanistic explanations for experimental human infections. To be submitted to ***Epidemiology and Infection.*** (IF=2.365, Ranking in Public, Environmental and Occupational Health = 39/122 = 31.97%)

本計畫發表國內外研討會

Szu-Chieh Chen, Chung-Min Liao. 2008. Evaluation of influenza viral kinetics and exhaled droplet size on indoor transmission dynamics. EPIDEMICS, First International Conference on Infectious Disease Dynamics, December 1-3, 2008.

王芊樺、**陳詩潔**、游舒涵、龔冠瑜、謝孟桓、王凱淞。咳嗽與說話飛沫粒徑特性研究。2010 環境與室內空氣品質研討會 (中華民國環境工程學會)，屏東。中華民國九十九年十一月十二日、十三日。

陳詩潔、劉靜宜、李思萱、周筱函、蔡一鳴、龔冠瑜。2009。流感病毒動態於人體肺部之研析。2009 台灣公共衛生學會。台北。中華民國九十八年十二月五、六日。

出席國際學術會議心得報告

計畫編號	NSC 97-2314-B-040 -006 -MY2
計畫名稱	室內呼吸性傳染病之傳輸潛能機率風險分析
出國人員姓名 服務機關及職稱	中山醫學大學 公共衛生學系(所) 陳詩潔 助理教授
會議時間地點	2-4 December 2009, Athens, Greece
會議名稱	EPIDEMICS^2 (Second International Conference on Infectious Disease Dynamics)
發表論文題目	

一、參加會議經過

第二屆 Epidemic 國際研討會於希臘雅典舉行，會場位於 Ledra Marriott Hotel。今年的會議規劃有別於去年，議程包括 (1) Learning epidemiology from sequence data (Chair: B. Korber), (2) Control (Chair: P. Piot), (3) Within host (Chair: M. Feinberg; A. Read), (4) Flu (Chair: M. Woolhouse; A. McLean), (5) Networks (Chair: J. A. P. Heesterbeek), (6) H1N1 (Chair: N. Ferguson; M. Woolhouse), (7) Evolution (Chair: S. Gurr), (8) Spational distribution of infectious diseases (Chair: R. Colwell), (9) Infections of wildlife (Chair: P. Walsh), and (10) Infections of livestock (Chair: J. A. P Heesterbeek)，亦增加了今年於全球所流行的新型流感 H1N1 的探討。

本人所投稿的議題於十二月上午八點半至四日上午以海報方式呈現，並與有興趣之學者相互討論切磋。與會者多為英國與美國學者，主題多在新型 H1N1 流感、肺結核、愛滋病、禽流感、肝炎及萊姆病等傳染病，而內容除了利用實驗結果結合模式參數之模擬，還有大規模全國性的數學模擬結果。議程安排部分，十二月二日、三日早上分別邀請幾位英國牛津大學學者(A. McLean; S. Gurr) 與美國 Los Alamos National Institute 人員蒞臨演講，可見此研討會於政府單位之重視程度。

二、與會心得

本次所舉辦的國際研討會，本人給予相當正面的評價，整體規劃可看出主辦單位之用心，與會者也幾乎 95%全程參與，除了議會期間聽述口頭報告之外，在中場休息之餘，也能與不同學者進行學術交流，如北京大學地理系的碩三研究生梁璐，討論 GIS 於登革熱的模擬與利用。海報展示區部分，提供學者討論的場地與空間，雖然舉辦時間為下午四點至六點，但輕鬆氣氛下與其他作者相談甚歡，與會者皆踴躍發問。本次研討會所攜回資料，包括各議程投稿作者與題目、相關領域且有興趣之海報影本，亦附上各通訊作者之職稱單位與電子信箱資料，以及 EPIDEMICS 期刊一本 (Volume 1, Number 3, September 2009) ，以利後續學術交流。

附件一 海報題目與摘要

Assessing the role of climate factors impact in dengue incidence in subtropical Taiwan

S. C. Chen[1] and C. M. Liao[2, *]
S.C. Chen[1,*], H.H. Chou[1], and C.M. Liao[2]

[1]Department of Public Health, College of Health Care and Management, Chung Shan Medical University, No. 110, Sec. 1, Chien-kuo N Road, Taichung 40242, Taiwan, ROC. [2]Department of Bioenvironmental Systems Engineering, National Taiwan University, Taipei, Taiwan 10617 ROC.

[*]Corresponding Author: e-mail: Tel.: +886-4-2473-0022*11792; Fax.: +886-4-2324-8179; scchen@csmu.edu.tw

Abstract

Introduction: Several researches indicated that the climate change may play an important impact in the incidence rate of mosquito-borne disease. Literature review evident that dengue fever shows a clear weather-related pattern in that rainfall and temperatures affect both the spread of mosquito vectors.

Methods: This study was conducted in Kaohsiung and Taipei because of the major dengue epidemic in southern Taiwan and the latest focus epidemic area in northern Taiwan, respectively. Monthly dengue incidence ratios (1/100,000) were estimated from monthly confirmed dengue cases over the specific-year end population size. We obtained the weekly maximum, mean, and minimum temperature, amount of rainfall, and relative humidity from 2001 to 2008. We redefined the frequency of monthly BI level > 2 (BI level > 2 (%)) to express the potential transmission frequency. We used cross-correlation and carried out a lagged cross-correlation analysis to study lagged effects of the climate variables on dengue incidence. Then, a generalized Poisson regression analyses is used to identify particular combinations of variables that results in the greatest explained variance of the dependent variable.

Results: Our result confirmed that temperature play a role on dengue incidence ratio in Taipei and Kaohsiung. Mean, maximum, and minimum temperatures have lags of 1 month and 2 months for Taipei and Kaohsiung, respectively. However, the rainfall has no lag effect in Taipei. Significantly impacts of maximum temperature and lag times implicated the key determinants in Kaohsiung by Poisson regression analysis.

Key words: Dengue fever, Rainfall, Temperature, Mosquito-borne disease, Taiwan

無研發成果推廣資料

97 年度專題研究計畫研究成果彙整表

計畫主持人：陳詩潔	計畫編號：97-2314-B-040-006-MY2
計畫名稱：室內呼吸性傳染病之傳輸潛能機率風險分析	

成果項目			量化			單位	備註（質化說明：如數個計畫共同成果、成果列為該期刊之封面故事...等）
			實際已達成數（被接受或已發表）	預期總達成數(含實際已達成數)	本計畫實際貢獻百分比		
國內	論文著作	期刊論文	0	0	100%	篇	
		研究報告/技術報告	0	0	100%		
		研討會論文	2	2	100%		1. 王芊樺、陳詩潔、游舒涵、龔冠瑜、謝孟桓、王凱淞。咳嗽與說話飛沫粒徑特性研究。2010 環境與室內空氣品質研討會（中華民國環境工程學會），屏東。中華民國九十九年十一月十二日、十三日。 2. 陳詩潔、劉靜宜、李思萱、周筱函、蔡一鳴、龔冠瑜。2009。流感病毒動態於人體肺部之研析。2009 台灣公共衛生學會。台北。中華民國九十八年十二月五、六日。
		專書	0	0	100%		
	專利	申請中件數	0	0	100%	件	
		已獲得件數	0	0	100%		
	技術移轉	件數	0	0	100%	件	
		權利金	0	0	100%	千元	
	參與計畫人力（本國籍）	碩士生	1	1	100%	人次	
		博士生	0	0	100%		
		博士後研究員	0	0	100%		
		專任助理	0	0	100%		

國外	論文著作	期刊論文	1	2	100%	篇	1. Chen SC, Liao CM. 2010. Probabilistic indoor transmission modeling for influenza (sub)type viruses. Journal of Infection 60(1): 26-35. (SCI) 2. Chen SC, You SH, Liu CY, Chio CP, Liao CM. A parsimonious viral dynamic model in epithelial cells enhances mechanistic explanations for experimental human infections. To be submitted to Epidemiology and Infection. (SCI)
		研究報告/技術報告	0	0	100%		
		研討會論文	1	1	100%		1. Szu-Chieh Chen, Chung-Min Liao. 2008. Evaluation of influenza viral kinetics and exhaled droplet size on indoor transmission dynamics. EPIDEMICS, First International Conference on Infectious Disease Dynamics, December 1-3, 2008.
		專書	0	0	100%	章/本	

	專利	申請中件數	0	0	100%	件	
		已獲得件數	0	0	100%		
	技術移轉	件數	0	0	100%	件	
		權利金	0	0	100%	千元	
	參與計畫人力（外國籍）	碩士生	1	1	100%	人次	
		博士生	0	0	100%		
		博士後研究員	0	0	100%		
		專任助理	0	0	100%		
其他成果 (無法以量化表達之成果如辦理學術活動、獲得獎項、重要國際合作、研究成果國際影響力及其他協助產業技術發展之具體效益事項等，請以文字敘述填列。)		無					

	成果項目	量化	名稱或內容性質簡述
科教處計畫加填項目	測驗工具(含質性與量性)	0	
	課程/模組	0	
	電腦及網路系統或工具	0	
	教材	0	
	舉辦之活動/競賽	0	
	研討會/工作坊	0	
	電子報、網站	0	
	計畫成果推廣之參與（閱聽）人數	0	

國科會補助專題研究計畫成果報告自評表

請就研究內容與原計畫相符程度、達成預期目標情況、研究成果之學術或應用價值（簡要敘述成果所代表之意義、價值、影響或進一步發展之可能性）、是否適合在學術期刊發表或申請專利、主要發現或其他有關價值等，作一綜合評估。

1. 請就研究內容與原計畫相符程度、達成預期目標情況作一綜合評估 ■達成目標 □未達成目標（請說明，以 100 字為限） □實驗失敗 □因故實驗中斷 □其他原因 說明：
2. 研究成果在學術期刊發表或申請專利等情形： 論文：■已發表 □未發表之文稿 □撰寫中 □無 專利：□已獲得 □申請中 ■無 技轉：□已技轉 □洽談中 ■無 其他：(以 100 字為限) 一篇發表一篇撰寫中

3. 請依學術成就、技術創新、社會影響等方面，評估研究成果之學術或應用價值（簡要敘述成果所代表之意義、價值、影響或進一步發展之可能性）（以500 字為限）

學術成就

本計畫提供一個預測性模式以模擬易感族群之流感傳輸潛能，以整合流感病毒動態模式、室內氣膠傳輸模式及飛沫粒徑分佈特性。藉由流感病毒動態模式，人體宿主和病原體之間交互作用可分為三個等級(上皮細胞、人體免疫反應與病毒力價)，評估每日時變的病毒力價產生率與飛沫粒徑大小；進而利用 Wells-Riley 方程式推求重要的參數感染風險(P)和基本再生數(R0)以量化流感傳輸潛能。結果顯示，病毒力價在感染後第二天達最大值，第七天達到 5.96×109 的 virions 病毒粒子數。流感病毒感染速率 P 和 R0 的中位數和 95%信賴區間分別為 0.132（0.09 – 0.19）和 1.19（0.76 – 1.86)。

技術創新

本計畫提供一個預測性模式以模擬易感族群之流感傳輸潛能，以整合流感病毒動態模式、室內氣膠傳輸模式及飛沫粒徑分佈特性。

社會影響

本研究未來之應用性廣，若發生新興傳染病則可快速收集相關流行病學資料，並以模式量化相關控制策略之成效，考量工程控制(如增加通風率、空氣過濾網之使用)、個人呼吸防護具及結合公共衛生干預政策之成效(如疫苗、隔離方法及接觸追蹤方法)，以快速控制傳染病之發生。